PAPER

Virtual detector theory for strong-field atomic ionization

IOP Publishing Journal of Physics B: Atomic, Molecular and Optical Physics
J. Phys. B: At. Mol. Opt. Phys. **51** (2018) 084002 (9pp) https://doi.org/10.1088/1361-6455/aab5a4

Virtual detector theory for strong-field atomic ionization

Xu Wang[1], **Justin Tian**[2] **and J H Eberly**[2]

[1] Graduate School, China Academy of Engineering Physics, Beijing 100193, People's Republic of China
[2] Department of Physics and Astronomy, University of Rochester, Rochester, NY 14627, United States of America

E-mail: xwang@gscaep.ac.cn

Received 11 December 2017, revised 28 February 2018
Accepted for publication 9 March 2018
Published 27 March 2018

Abstract

A virtual detector (VD) is an imaginary device located at a fixed position in space that extracts information from the wave packet passing through it. By recording the particle momentum and the corresponding probability current at each time, the VDs can accumulate and build the differential momentum distribution of the particle, in a way that resembles real experiments. A mathematical proof is given for the equivalence of the differential momentum distribution obtained by the VD method and by Fourier transforming the wave function. In addition to being a tool for reducing the computational load, VDs have also been found useful in interpreting the ultrafast strong-field ionization process, especially the controversial quantum tunneling process.

Keywords: strong-field ionization, differential momentum distribution, quantum tunneling

1. Introduction

Ionization is one of the fundamental processes of strong-field light-atom interaction. It is the very first step of the well accepted recollision scenario [1, 2], which assumes that an electron is emitted via quantum tunneling before being accelerated in the laser field and possibly driven back to the parent ion to initiate various physical processes, including high harmonic generation [3, 4], nonsequential double or multiple ionization [5, 6], laser-induced electron diffraction [7, 8], etc. It is surprising, in retrospect, to see that a combination of the long familiar elements of atoms and photons could have led to so much new physics [9, 10], and pushed us into the unprecedented attosecond time domain [11].

Theoretical understanding of the interaction between a strong laser field and an atomic or molecular target relies heavily on numerical wave function calculations due to the nonperturbative nature of the interaction. Such a calculation usually imposes a heavy computational load, especially when differential information is of interest, due to the need for a large numerical grid to hold the wave function, which may spread to hundreds to thousands of atomic units in space driven by the strong laser field. The computational load quickly becomes infeasible as the number of electrons increases. In fact, many strong-field time-dependent Schrödinger equation (TDSE) calculations are still based on the single-active-electron approximation using an effective potential describing the remaining ion core [12–15]. *Ab initio* calculations on the helium atom interacting with strong (extreme ultraviolet to near infrared) laser fields have been performed by a few groups using supercomputers [16–20]. However, there is no near-future prospect of extending such calculations beyond helium.

Attempts have been made to reduce the computational load based on the observation that at large distances from the ion core, the effect of the Coulomb potential is weak, and the electron motion can be approximated as a free particle driven by the laser field. Such motion can be described analytically by a Volkov state [21], and then further numerical integrations are not needed. Examples based on this approximation include a time-dependent surface flux method proposed by Scrinzi *et al* [22, 23], and an analytical *R*-matrix method proposed by Smirnova *et al* [24–26].

Another method, called a virtual detector (VD) method, proposed by Feuerstein and Thumm in the strong-field regime [27], presents a different idea of approaching the same goal of reducing the computation load. Instead of seeking more economic ways of calculating or approximating the wave function evolving to the end of the laser pulse, the VD method seeks the possibility of extracting desired information (e.g., electron momentum distribution) from the wave function as early as possible, long before the end of the pulse.

After desired information has been extracted, further evolution of the wave function is no longer of concern and it can be destroyed by an absorbing boundary condition. No large numerical grid is thus needed to hold the ever spreading wave function. Based on the VD method, Wang *et al* developed a hybrid quantum mechanical and classical trajectory approach that takes full account of the long range ion-core Coulomb potential, and the VD method has been shown to agree very well with ultrashort laser pulse TDSE results [28].

In addition to being a tool of reducing the computational load, the VD method was recently found useful in helping to interpret and characterize the tunneling ionization process, which is known to be controversial. For example, Teeny *et al* [29, 30] and Ni *et al* [31, 32] use the VD method to extract tunneling-ionization-related information such as tunneling time, tunneling rate, position of tunneling exit, etc. Tian *et al* [33] use it to solve the apparent controversy of electron longitudinal momentum at the tunneling exit [34–37]. Considering that quantum tunneling is the first step of the recollision scenario, and that widely used recollision-based semiclassical models [38–44] employ explicitly the tunneling parameters (the position of the tunneling exit and the electron momentum at the tunneling exit) as the initial conditions for subsequent classical trajectory evolutions, clear interpretation and precise characterization of the tunneling process is useful and important for recollision physics.

This special issue article has two goals. The first goal is to give an introduction to the VD method as well as a brief review of some published works based on it. We believe such an introduction and review will be beneficial for those who are interested in this method. The second goal is to present some new results. Specifically, we give a mathematical proof to a basic conjecture of the VD method that the differential momentum distribution obtained using the VD method is equivalent to that obtained from Fourier transforming the wave function. Until now, that conjecture has only been proved by Feuerstein and Thumm for the special case of one-dimensional free-particle Gaussian wave packets [27].

This article is organized as follows. In section 2 an introduction to the VD method is given. In section 3 the special situation of free-particle wave packets is discussed, and the proof to the conjecture just mentioned is given in an asymptotic limit. In section 4 the VDs are moved from the asymptotic limit to the vicinity of the interaction center, where they are found useful in helping to interpret the strong-field tunneling ionization process. Finally a summary is given in section 5.

2. The VD method

2.1. Basic idea of the VD method

A VD is an imaginary device located at some fixed position in space and extracting information from the wave function passing through it. The information of interest usually includes the particle velocity or momentum (the exact meaning of which will be explained in detail later) and the probability current. This is the same as a real detector located at some fixed position in space and detecting the probability current passing through it.

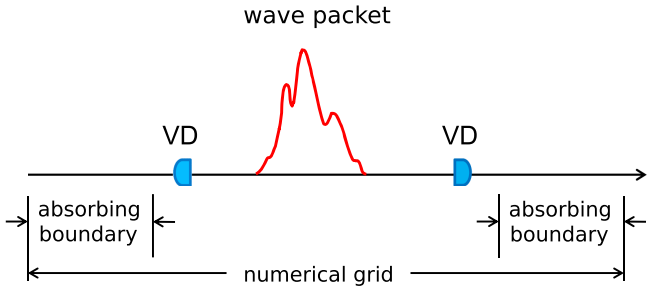

Figure 1. Illustration of the virtual detector method in one dimension. A wave packet is created near the center of the numerical grid. A VD is placed each side, extracting information from the wave packet. After passing through the VDs, the wave enters the absorbing boundary zone being absorbed.

The differences between a VD and a real detector are also obvious. First, a virtual detection process is just an imaginary information-extracting process so it does not affect the wave function. A real detection process has to involve some sort of interaction with a classical apparatus and results of this interaction changes the wave function. Second, a VD can be put anywhere in space, e.g., microscopically close to an interaction center, whereas a real detector always has a macroscopic distance from the interaction center. The freedom of putting a VD microscopically close to the interaction center has been exploited to extract dynamical information about the tunneling ionization process, as will be discussed in section 4. Third, a VD avoids the complications of a real detector, such as detection efficiency, random noise, response time, etc.

The original goal of the VD method was to reduce the computational load of obtaining differential momentum distributions in strong-field processes, such as molecular dissociation, atomic ionization, etc [27]. After information extraction by the VDs, further wave function evolution is not of concern so that it can be destroyed via an absorbing boundary. (Of course this implies that the wave function should not be substantially altered in later evolutions, such as encountering a recollision process. A later recollision can be avoided by either putting the VDs far enough from the ion core or using elliptical polarization.) Therefore a large numerical grid is not needed to keep the whole wave function, which can spread to a distance of hundreds to thousands of atomic units.

A schematic illustration of the VD method is shown in figure 1 for one dimension, and extension to two or three dimensions is conceptually straightforward. A wave packet is created in the interaction center, via strong-field ionization, and it evolves as a function of time. A VD is placed on each side to extract information from the wave packet. After passing through the VDs, the wave packet enters the absorbing boundary zone and is absorbed (destroyed) to avoid reflection.

2.2. Flow velocity of the probability fluid

A VD records particle velocity (momentum) from the wave packet. This velocity is understood as the flow velocity of the

probability fluid. If we write a wave function in the polar form

$$\Psi(\vec{r}, t) = A(\vec{r}, t)\mathrm{e}^{\mathrm{i}\phi(\vec{r},t)}, \tag{1}$$

with $A(\vec{r}, t)$ and $\phi(\vec{r}, t)$ real functions and $A(\vec{r}, t) \geqslant 0$, then the probability density is

$$\rho(\vec{r}, t) = |\Psi(\vec{r}, t)|^2 = A(\vec{r}, t)^2, \tag{2}$$

and the probability current can be written

$$\begin{aligned}\vec{j}(\vec{r}, t) &= \frac{\mathrm{i}\hbar}{2m}[\Psi(\vec{r}, t)\nabla\Psi^*(\vec{r}, t) - \text{c.c.}] \\ &= \rho(\vec{r}, t)\frac{\hbar}{m}\nabla\phi(\vec{r}, t).\end{aligned} \tag{3}$$

In analogy to the classical fluid equation $\vec{j}(\vec{r}, t) = \rho(\vec{r}, t)\vec{v}(\vec{r}, t)$, one sees that the flow velocity is proportional to the spatial gradient of the phase of the wave function

$$\vec{v}(\vec{r}, t) = \frac{\hbar}{m}\nabla\phi(\vec{r}, t), \quad \text{or} \tag{4}$$

$$\vec{p}(\vec{r}, t) = \hbar\nabla\phi(\vec{r}, t), \quad \text{or} \tag{5}$$

$$\vec{k}(\vec{r}, t) = \nabla\phi(\vec{r}, t). \tag{6}$$

These are the velocity/momentum/wave number formulas extracted by a VD located at position $\vec{r}$ at time t. We emphasize that it is meaningful to talk about the flow velocity at a fixed position, and the VD method is therefore closely related to the field of quantum hydrodynamics [45] and trajectory formalisms of quantum mechanics [46–49].

Another way of obtaining the flow velocity is to apply the momentum operator to the wave function

$$\begin{aligned}\hat{p}\Psi(\vec{r}, t) &= -\mathrm{i}\hbar\nabla\Psi(\vec{r}, t) \\ &= \left[\hbar\nabla\phi(\vec{r}, t) - \mathrm{i}\hbar\frac{\nabla A(\vec{r}, t)}{A(\vec{r}, t)}\right]\Psi(\vec{r}, t).\end{aligned} \tag{7}$$

The velocity associated to the real part is exactly the flow velocity of equation (4), and the velocity associated to the imaginary part is called the Einstein osmotic velocity, related to quantum diffusion.

In the VD method, at each time step the probability density $\rho(\vec{r}, t)$, which contains the amplitude information of the wave function, and the probability current $\vec{j}(\vec{r}, t)$, which contains the phase information of the wave function, are recorded. And it is known from quantum mechanics that knowing the probability density and the probability current is equivalent to knowing the amplitude and the phase of the wave function, up to a constant overall phase [50]. Therefore in principle the VD method is able to obtain all the physical information carried by a wave function at the time of (virtual) detection.

2.3. Flow velocity in momentum space

To have a better understanding about the flow velocity of the probability fluid, we give its expression in momentum space. Assume a wave packet is created at time $t = 0$, when it can be written as

$$\Psi(\vec{r}, t = 0) = \frac{1}{(2\pi)^{3/2}}\int\tilde{\psi}(\vec{k})\mathrm{e}^{\mathrm{i}\vec{k}\cdot\vec{r}}\mathrm{d}^3\vec{k}. \tag{8}$$

Then the wave packet evolves with time according to

$$\Psi(\vec{r}, t) = \frac{1}{(2\pi)^{3/2}}\int\tilde{\psi}(\vec{k})\mathrm{e}^{\mathrm{i}\Delta(\vec{k},\vec{r},t)}\mathrm{d}^3\vec{k}, \tag{9}$$

where we have defined

$$\Delta(\vec{k}, \vec{r}, t) \equiv \vec{k}\cdot\vec{r} - \omega(\vec{k})t \tag{10}$$

with $\omega(\vec{k})$ the dispersion relation.

From equations (1) and (9), we can get

$$\mathrm{e}^{\mathrm{i}\phi(\vec{r},t)} = \frac{1}{A(\vec{r}, t)}\frac{1}{(2\pi)^{3/2}}\int\tilde{\psi}(\vec{k})\mathrm{e}^{\mathrm{i}\Delta(\vec{k},\vec{r},t)}\mathrm{d}^3\vec{k}. \tag{11}$$

Take logarithms of both sides and we get

$$\begin{aligned}\mathrm{i}\phi(\vec{r}, t) = \ln\left\{\int\tilde{\psi}(\vec{k})\mathrm{e}^{\mathrm{i}\Delta(\vec{k},\vec{r},t)}\mathrm{d}^3\vec{k}\right\} \\ - \ln A(\vec{r}, t) - \ln(2\pi)^{3/2}.\end{aligned} \tag{12}$$

Then take the spatial gradient of the phase function

$$\nabla\phi(\vec{r}, t) = \frac{\int\vec{k}\tilde{\psi}(\vec{k})\mathrm{e}^{\mathrm{i}\Delta(\vec{k},\vec{r},t)}\mathrm{d}^3\vec{k}}{\int\tilde{\psi}(\vec{k})\mathrm{e}^{\mathrm{i}\Delta(\vec{k},\vec{r},t)}\mathrm{d}^3\vec{k}} + \mathrm{i}\frac{\nabla A(\vec{r}, t)}{A(\vec{r}, t)}. \tag{13}$$

Because $\phi(\vec{r}, t)$ and $A(\vec{r}, t)$ are both real functions, we conclude that the imaginary part of the first term on the right hand side must cancel the second term (the proof will not be shown here). Then we have

$$\nabla\phi(\vec{r}, t) = \mathrm{Re}\left\{\frac{\int\vec{k}\tilde{\psi}(\vec{k})\mathrm{e}^{\mathrm{i}\Delta(\vec{k},\vec{r},t)}\mathrm{d}^3\vec{k}}{\int\tilde{\psi}(\vec{k})\mathrm{e}^{\mathrm{i}\Delta(\vec{k},\vec{r},t)}\mathrm{d}^3\vec{k}}\right\}. \tag{14}$$

We see that formally $\nabla\phi(\vec{r}, t)$ is the real part of the average value of $\vec{k}$, consistent with the interpretation given by equation (7) in real space.

2.4. Probability current in momentum space

From equations (2) and (9), the probability density can be written in the form

$$\begin{aligned}\rho(\vec{r}, t) = \frac{1}{(2\pi)^3}\int\tilde{\psi}(\vec{k})\mathrm{e}^{\mathrm{i}\Delta(\vec{k},\vec{r},t)}\mathrm{d}^3\vec{k} \\ \times\int\tilde{\psi}^*(\vec{k})\mathrm{e}^{-\mathrm{i}\Delta(\vec{k},\vec{r},t)}\mathrm{d}^3\vec{k}.\end{aligned} \tag{15}$$

From equations (3), (14), and (15), the probability current can be shown as

$$\begin{aligned}\vec{j}(\vec{r}, t) = \frac{1}{(2\pi)^3}\frac{\hbar}{m}\mathrm{Re}\left\{\int\vec{k}\tilde{\psi}(\vec{k})\mathrm{e}^{\mathrm{i}\Delta(\vec{k},\vec{r},t)}\mathrm{d}^3\vec{k}\right. \\ \left.\times\int\tilde{\psi}^*(\vec{k})\mathrm{e}^{-\mathrm{i}\Delta(\vec{k},\vec{r},t)}\mathrm{d}^3\vec{k}\right\}.\end{aligned} \tag{16}$$

We see that further evaluations of the flow velocity and the probability current involve the following two integrals

$$I_1 = \int \tilde{\psi}(\vec{k}) e^{i\Delta(\vec{k},\vec{r},t)} d^3\vec{k}, \tag{17}$$

$$I_2 = \int \vec{k}\tilde{\psi}(\vec{k}) e^{i\Delta(\vec{k},\vec{r},t)} d^3\vec{k}, \tag{18}$$

or their complex conjugates, which in general have to be evaluated numerically.

3. Free-particle wave packets and the asymptotic limit

The formalism presented in the previous section is general and exact. No approximations have been made. In this section we consider the special case of free-particle wave packets for the following reasons: first, free-particle wave packets relate closely to real detection processes because a real detector always has a macroscopic distance from the interaction center and the particles can be regarded as free at the time of detection. Second, free-particle wave packets provide the possibility of analytical insights into the VD method itself.

Let us consider a free-particle wave packet by specifying the dispersion relation

$$\omega(\vec{k}) = \frac{\hbar k^2}{2m}, \tag{19}$$

which makes the phase given in equation (10) quadratic in $\vec{k}$. Completing the square, one gets

$$\Delta(\vec{k}, \vec{r}, t) = -\frac{\hbar t}{2m}\left(\vec{k} - \frac{m\vec{r}}{\hbar t}\right)^2 + \frac{mr^2}{2\hbar t}. \tag{20}$$

3.1. The asymptotic limit

Further evaluations of the two integrals in equations (17) and (18) are simple in an asymptotic limit where t is large. The term $e^{i\Delta(\vec{k},\vec{r},t)}$ is highly oscillatory except in the vicinity of the stationary wave vector

$$\vec{k}_s = \frac{m\vec{r}}{\hbar t}. \tag{21}$$

Recall that $\vec{r}$ is the location of the VD. In this asymptotic limit I_1 and I_2 can be evaluated simply

$$I_1 = \tilde{\psi}(\vec{k}_s)\exp\left(i\frac{mr^2}{2\hbar t}\right)\left(\frac{2\pi m}{\hbar t}\right)^{3/2} e^{-i\frac{3\pi}{4}}, \tag{22}$$

$$I_2 = \vec{k}_s I_1. \tag{23}$$

We have used the Fresnel integral

$$\int e^{\pm ibx^2} d^3\vec{x} = \left(\frac{\pi}{b}\right)^{3/2} e^{\pm i\frac{3\pi}{4}}, \text{ for } b > 0. \tag{24}$$

The asymptotic limit and the stationary-phase condition effectively disentangle the wave vector superpositions appearing in equations (17) and (18).

Using equation (14) the flow velocity becomes

$$\vec{v}(\vec{r}, t) = \frac{\hbar}{m}\nabla\phi(\vec{r}, t) = \frac{\hbar}{m}\mathrm{Re}\left(\frac{I_2}{I_1}\right) = \frac{\hbar\vec{k}_s}{m} = \frac{\vec{r}}{t}, \tag{25}$$

which is just the classical velocity for the particle flying from the interaction center (where the wave packet is created) to the VD.

Using equation (16) the probability current becomes

$$\begin{aligned}\vec{j}(\vec{r}, t) &= \frac{1}{(2\pi)^3}\frac{\hbar}{m}\mathrm{Re}(I_1^* I_2) \\ &= \left(\frac{m}{\hbar}\right)^3 \frac{\vec{r}}{t^4}\left|\tilde{\psi}\left(\frac{m\vec{r}}{\hbar t}\right)\right|^2 \\ &= \left(\frac{m}{\hbar}\right)^2 \frac{1}{t^3}\vec{k}_s\,|\tilde{\psi}(\vec{k}_s)|^2.\end{aligned} \tag{26}$$

This formula links the probability current detected by a VD at position $\vec{r}$ and time t, with the Fourier component $|\tilde{\psi}(\vec{k}_s)|^2$ of the wave packet. It provides a practical way of obtaining the Fourier components of free-particle wave packets.

3.2. The differential momentum distribution

A VD, located at position $\vec{r}$, detects at each time t the flow momentum of the wave passing through it, as well as the probability current, which is used as the weight of the corresponding momentum. By accumulating the momentum and the corresponding weight over time, one obtains the differential momentum distribution. We now prove that the momentum distribution obtained this way, a scheme that resembles real experiments, is equivalent to Fourier transforming the free-particle wave packet.

The total probability of particle detection is

$$\int_0^\infty [\vec{j}(\vec{r}, t)\cdot d\vec{S}]dt = \int [\vec{j}(\vec{r}, \vec{k}_s)\cdot d\vec{S}]\left|\frac{dt}{d^3\vec{k}_s}\right| d^3\vec{k}_s, \tag{27}$$

where $d\vec{S} = \hat{r}dS = \hat{r}r^2 d\Omega$ is the area element of the detector, with $d\Omega$ the spanned solid angle. The probability density of finding a particle within a small momentum volume $d^3\vec{k}_s$ around $\vec{k}_s$ is

$$\begin{aligned}P(\vec{k}_s) &= [\vec{j}(\vec{r}, \vec{k}_s)\cdot d\vec{S}]\left|\frac{dt}{d^3\vec{k}_s}\right| \\ &= j(\vec{r}, \vec{k}_s)r^2 d\Omega\left|\frac{dt}{k_s^2 dk_s d\Omega}\right|.\end{aligned} \tag{28}$$

Using the stationary-phase relation given by equation (21), we have

$$\frac{\mathrm{d}t}{\mathrm{d}k_s} = -\frac{mr}{\hbar k_s^2}. \tag{29}$$

Then the differential momentum distribution of equation (28), after straightforward algebra, becomes precisely

$$P(\vec{k}_s) = |\tilde{\psi}(\vec{k}_s)|^2. \tag{30}$$

We have finished our proof that in the asymptotic limit, the differential momentum distribution obtained by the VD method is equivalent to Fourier transforming the free-particle wave packet.

3.3. One-dimensional Gaussian wave packet

In this subsection we use a 1D Gaussian wave packet to illustrate the flow velocity, the probability current, and the asymptotic limit. The purpose is to help the reader to better understand these physical quantities. For the sake of convenience, we consider an electronic wave packet and use atomic units, so $\hbar = m = 1$.

Consider a Gaussian wave packet with spatial width Γ at time $t = 0$

$$\Psi(x, t = 0) = \frac{1}{\sqrt{\Gamma}\,\pi^{1/4}} \exp\left(-\frac{x^2}{2\Gamma^2}\right) \exp(\mathrm{i}k_0 x), \tag{31}$$

which is centered at $x = 0$ and moves with group velocity k_0. The corresponding Fourier transform is

$$\tilde{\psi}(k) = \frac{\sqrt{\Gamma}}{\pi^{1/4}} \exp\left[-\frac{\Gamma^2}{2}(k - k_0)^2\right]. \tag{32}$$

Using the 1D version of equations (14), (17)–(19), we easily get

$$k(x, t) = \frac{\partial \phi(x, t)}{\partial x} = \mathrm{Re}\left(\frac{I_2}{I_1}\right) = \frac{\Gamma^4 k_0 + xt}{\Gamma^4 + t^2}, \tag{33}$$

which is the same as equation (14) of [27] using a different approach. Note that this expression is valid for all t since the asymptotic limit has not been applied. We see that in the zero-time limit, $k(x, t = 0) = k_0$, which is the group velocity of the wave packet, and in the asymptotic limit $k(x, t \to \infty) = x/t$, which is the classically expected velocity. We also see that the asymptotic limit is fulfilled when the following two conditions are met: $xt \gg \Gamma^4 k_0$ and $t^2 \gg \Gamma^4$. Or we can combine them as $t \gg \max\{\Gamma^2, \Gamma^4 k_0/x\}$.

An illustration of $k(x, t)$ is given in figure 2 for a fixed VD position $x = 20$ a.u. The parameters of the wave packet are chosen as $k_0 = 2$ a.u., $\Gamma = 1$ a.u. (panel (a)) and $\Gamma = 2$ a.u. (panel (b)). The red (solid) curve in each panel is the velocity detected by the VD as a function of time, viz. $k(x, t)$ given by equation (33). The blue (dashed) curve in each panel is the classically expected velocity, given by x/t. When the asymptotic condition is met, the velocity detected by the VD approaches the classical velocity. One can check that the asymptotic condition for each case is $t \gg 1$ a.u. and $t \gg 4$ a.u., respectively. It is worth mentioning that in the asymptotic limit the time t does not have to be macroscopic.

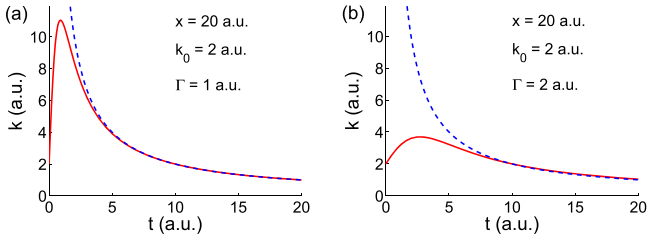

Figure 2. Velocity detected by a VD located at $x = 20$ a.u. The Gaussian wave packet is moving with a group speed $k_0 = 2$ a.u. The initial width of the wave packet is $\Gamma = 1$ a.u. (a) and $\Gamma = 2$ a.u. (b). The red solid curve in each panel is the velocity detected by the VD, given by equation (33). The blue dashed curve in each panel is the classically expected velocity x/t.

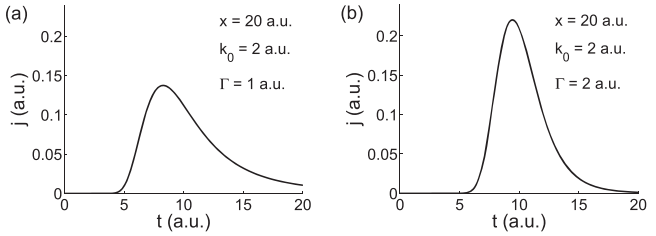

Figure 3. Probability current detected by a VD located at $x = 20$ a.u. as a function of time, corresponding to the same two cases as figure 2.

For $t = 0$, we have $k = k_0$ and is independent of the position of the VD. Before reaching the asymptotic limit where a single Fourier component dominates due to the stationary-phase condition, the velocity detected by the VD, according to equation (14), is the result of the superposition of all Fourier components.

Using the 1D version of equation (16) the probability current can be obtained simply

$$j(x, t) = \frac{1}{2\pi}\frac{\hbar}{m}\mathrm{Re}(I_1^* I_2) = \frac{\Gamma k(x, t)}{\sqrt{\pi(\Gamma^4 + t^2)}} \exp\left[-\frac{\Gamma^2 (x - k_0 t)^2}{\Gamma^4 + t^2}\right], \tag{34}$$

where $k(x, t)$ is given by equation (33). This result is the same as equation (16) of [27]. Figure 3 shows the probability current passing through the VD corresponding to the two cases of figure 2. Since the VD locates at $x = 20$ a.u. and the wave packet moves with a group velocity of $k_0 = 2$ a.u., one expects a peak probability current around $t = 10$ a.u. Because the wave packet in the first case (with $\Gamma = 1$ a.u.) is initially more localized in space than the second case (with $\Gamma = 2$ a.u.), we expect the first wave packet to spread more quickly than the second one. Therefore the probability current shown in panel (a) starts earlier and ends later in time than the one shown in panel (b).

3.4. Free-particle wave packet in a laser field

In a strong-field experiment the interaction between the laser field and the atomic or molecular target happens in the laser focus. Interaction resultants, such as emitted electrons, ionized atoms, molecular fragments, etc, fly out from the laser focus to the detector, which has a macroscopic distance from the laser focus. The detection happens long after (∼nanoseconds) the laser pulse (∼femtoseconds) is over. In fact, during a laser pulse of a few tens of femtoseconds, the resultants are deep inside the focus, having little chance of experiencing the spatial gradient of the laser focus before the laser pulse is over.

A VD, in contrast, has the flexibility of being put anywhere in space, including places inside the laser focus. For the VD method to be useful in reducing the computational load of strong-field processes, the VDs have to be put inside the laser focus, with distances from the interaction center much smaller than the length of the numerical grid needed to keep the whole wave function. Therefore it is important to understand what is detected by a VD inside a laser field.

We consider here the simplest situation that a free-particle wave packet is created at time $t = 0$ inside a laser field (which may not be zero then). Then the theory and formalism given previously apply to the current situation, provided that some modifications are made. Specifically, the dispersion relation in equation (19) needs to be modified to

$$\omega(\vec{k}, t) = \frac{1}{2\hbar m}[\hbar\vec{k} - q\vec{\mathcal{A}}(t)]^2, \tag{35}$$

where q is the charge of the particle and $\vec{\mathcal{A}}(t)$ is the vector potential of the laser field. The spatial dependence of the vector potential is not considered due to the reason just explained above.

The phase of equation (20) becomes (with a subscript L denoting laser)

$$\begin{aligned}\Delta_L(\vec{k}, \vec{r}, t) &= \vec{k}\cdot\vec{r} - \int_0^t \omega(\vec{k}, t')\mathrm{d}t' \\ &= \vec{k}\cdot\vec{r} - \frac{\hbar k^2 t}{2m} + \vec{k}\cdot\frac{q}{m}\int_0^t \vec{\mathcal{A}}(t')\mathrm{d}t' \\ &\quad - \frac{q^2}{2\hbar m}\int_0^t \mathcal{A}^2(t')\mathrm{d}t' \\ &\equiv \vec{k}\cdot\vec{r} - \frac{\hbar k^2 t}{2m} + \vec{k}\cdot\vec{l}\,(t) + \xi(t).\end{aligned} \tag{36}$$

Two short-hand notations $\vec{l}\,(t)$ and $\xi(t)$ are introduced, whose definitions can be seen comparing the third step with the second step. The first two terms on the right hand side are the same as those of the no-laser situation, and the additional two terms are introduced by the laser field. $\vec{l}\,(t)$ has the units of length and is usually called the quiver displacement induced by the laser electric field from time 0 to t, and $\xi(t)$ is an additional phase usually called the ponderomotive phase.

In the asymptotic limit when t is large, the phase is highly oscillatory except in the vicinity of the stationary $\vec{k}$ vector, which, by requiring $\partial\Delta_L/\partial\vec{k} = 0$, is now

$$\vec{k}_s = \frac{m}{\hbar t}[\vec{r} + \vec{l}\,(t)]. \tag{37}$$

We see that the quiver displacement $\vec{l}\,(t)$ enters into the picture. As explained above, and demonstrated in figure 2, fulfilling the asymptotic condition does not necessarily conflict the configuration that the VDs are put inside the laser focus and close to the interaction center.

Following similar steps as in the no-laser case, we get the probability current detected by a VD located at $\vec{r}$ and at time t

$$\vec{j}\,(\vec{r}, t) = \left(\frac{m}{\hbar}\right)^2\frac{1}{t^3}\left[\vec{k}_s - \frac{q}{\hbar}\vec{\mathcal{A}}(t)\right]|\tilde{\psi}(\vec{k}_s)|^2, \tag{38}$$

which reduces to equation (26) as the laser field vanishes. Equation (38), together with equation (37), tells us how to decode the Fourier components of the free-particle wave packet from the probability current detected by the VDs, in the presence of a laser electric field.

4. Virtual detectors at the tunneling exit

In the previous section, we focus on the asymptotic limit where the particle wave packet is far from the interaction center and hence can be regarded as a free wave packet. We mathematically prove that in the asymptotic limit, the differential momentum distribution obtained by the VD method, a scheme that resembles real experiments, is equivalent to Fourier transforming the wave packet.

In this section we consider the opposite limit: putting a VD close to the interaction center to extract dynamical information especially about the tunneling ionization process. This kind of study is enabled by the freedom of the VD method, for no real detectors can be put microscopically close to an atom.

The theoretical studies reviewed in this section are motivated by two factors. The first is pure curiosity. The following questions have been asked, for example: (i) Does the electron need time to tunnel through a potential barrier? (ii) What is the velocity of the electron at the tunneling exit (i.e., right after finishing the tunneling process)? We believe that one understands the tunneling ionization process better if these questions are answered, instead of being simply dismissed. After all, how does one understand the tunneling ionization process without asking questions like these?

The second factor is the demand from experiments. Experiments have tried to answer the above-mentioned tunneling-ionization-related questions without being overburdened with theoretical debates. For example, attempts have been made to answer whether the electron emission has a time delay from the peak of the laser electric field [51–54]. For another example, attempts have also been made to answer whether there is a nonzero velocity of the electron at the tunneling exit [34–37]. These authors interpret their data partially based on classical arguments. It is not obvious what quantities in quantum mechanics correspond to what they want to retrieve. For example, what quantity in quantum

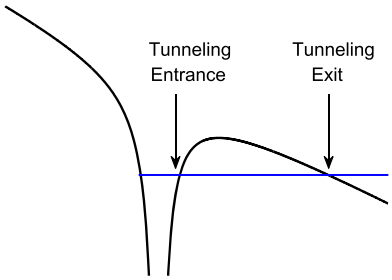

Figure 4. Illustration of tunneling entrance and tunneling exit in strong-field ionization. The black curve shows a tilted Coulomb potential in a laser electric field. The horizontal line shows the energy level of a bound state. The point of tunneling entrance and of tunneling exit can be well defined by the crossings of the energy level with the Coulomb potential barrier.

mechanics is the time delay between electron emission and the peak of the laser electric field? What quantity in quantum mechanics is the electron velocity at the tunneling exit?

The VD method provides a conceptually straightforward way of understanding the tunneling ionization process. Physical quantities that correspond to the experiments can be easily defined quantum mechanically using the VD concept. Next, we will review and briefly explain the use of the VD method in understanding the above-mentioned experiments on the tunneling ionization process.

4.1. Time delays in tunneling ionization

Several attempts have been made trying to answer the question whether tunneling ionization is instantaneous [51–54]. These experiments retrieve the time difference between the peak of the laser electric field and the peak of tunneling ionization, which is known to be extremely sensitive to the electric field strength. Elliptically polarized laser pulses are used which have two properties to exploit: first, there are two clear field peaks each laser cycle so the time of laser field peak is well defined; second, electrons emitted at different times fly to different spatial angles due to the rotating feature of elliptical polarization. By measuring the angular distribution of the emitted electron and assuming the electron motion is classical after emission, the ionization time can be retrieved.

One sees that the interpretation provided by these works [51–54] is largely based on classical mechanics. From the theoretical point of view, the first question to ask is probably: what quantity in quantum mechanics corresponds to the time delay between laser field peak and ionization?

Teeny *et al* show that this time delay can be straightforwardly defined quantum mechanically using the VD concept [29, 30]. By putting a VD at the tunneling exit (as illustrated in figure 4. Note that if the tunneling process is nonadiabatic, the location of the tunneling exit may not be so clearly defined.), the VD records the electron probability current as a function of time, and a clear peak can be identified denoted as $t_{\rm exit}$. The time delay that corresponds to the quantity retrieved by the experiment is $t_{\rm delay} = t_{\rm exit} - t_0$, where t_0 is the time of laser field peak. Teeny *et al* further show numerical results (see figure 4 of [30]) that this $t_{\rm delay}$ is not positive definite: it may vary between about ± 20 attoseconds depending on the laser electric field strength. This means that the electron may be most probably emitted shortly (on the attosecond time scale) before or after the peak of the laser electric field. The numerical results are in good agreement with the conclusion of the experiment.

By putting another VD at the tunneling entrance (as illustrated in figure 4) and recording the electron probability current there, one finds the latter quantity peaks at time $t_{\rm in}$. The time difference $t_{\rm tunneling} = t_{\rm exit} - t_{\rm in}$ is, we believe, the most straightforward quantity that corresponds to our understanding of the time that the electron needs to tunnel through the potential barrier. Teeny *et al* show that (see figure 4 of [30]) this $t_{\rm tunneling}$ is finite and positive definite, the precise value of which depends on the laser field strength. For lower field strengths, the potential barrier is thicker and the tunneling time is larger. And for higher field strengths, the potential barrier is thinner and the tunneling time is smaller. The absolute values of the tunneling time are on the order of 10–100 attoseconds for strong-field ionization.

4.2. Electron velocity at the tunneling exit

Another quantity that experiments [34–37] have tried to retrieve is the velocity of the electron at the tunneling exit point. This velocity is usually assumed to be zero based on the argument that at the tunneling exit the kinetic energy equals zero. And this zero-velocity assumption has been used as the initial condition of some widely used semiclassical models based on the three-step recollision spirit [38–44]. Note that here we are talking about the longitudinal velocity that is parallel to the laser polarization direction, whereas the transverse velocity perpendicular to the polarization direction is usually assumed to obey a Gaussian distribution centered at zero without much controversy [55, 56].

The retrieval of this longitudinal tunneling velocity is also based partly on classical mechanics: the electron motion is assumed to be classical after ionization. Pfeiffer *et al* show that if the velocity at the tunneling exit is assumed to be precisely zero, then the theoretically predicted end-of-pulse momentum distribution will have a relatively large discrepancy with the data. By adjusting the width of the tunneling exit velocity distribution (which, however, is still assumed to be centered at zero with a Gaussian shape) hence allowing nonzero velocities, a best fit to the data can be achieved. The authors show initially that a relatively large width of about 0.8 a.u. provides the best fit to the data [34]. But later this width was corrected by the same group to about 0.4 a.u. using a different data-analyzing method [35, 36].

Interestingly and puzzlingly for quite some time, the experiment by Sun *et al* [37] using the same retrieval procedure but a different atomic target (Kr versus He as used by Pfeiffer *et al*) reaches a different conclusion that the zero-velocity assumption is still good. They found that the tunneling exit velocity for Kr is narrowly centered at zero with a possible small uncertainty of about 0.1 a.u.

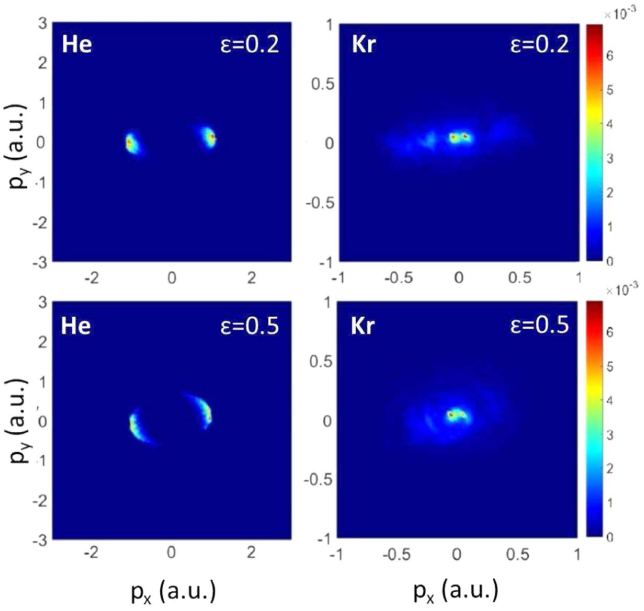

Figure 5. Tunneling-exit-point momentum distributions for He (left column) and Kr (right column). Two ellipticity values are used for each atom, as labeled on each panel. The laser intensity for He is 8×10^{14} W cm^{-2}, and for Kr 1.2×10^{14} W cm^{-2}.

Let us return to the apparent contradicting experimental conclusions a little later, but first ask the following question: what quantum mechanical quantity corresponds to this tunneling exit velocity? What does it mean by a velocity at a specified position? The flow velocity of the probability fluid, as extracted by a VD, provides possibly the only sensible quantum mechanical definition to the quantity retrieved in these two experiments.

Tian *et al* (the same authors of the current article) numerically study the problem of the tunneling exit velocity using the VD method [33]. By putting VDs in the vicinity of the tunneling exit points and recording the probability flow velocity and the corresponding weight (viz., the probability current) at each time, a differential momentum distribution can be obtained at the tunneling exit point (in contrast to experimentally measurable momentum distributions which are obtained in the asymptotic limit). These tunneling-exit-point differential momentum distributions are shown in figure 5 for He and Kr, using the same laser intensities as used in the experiments [34, 37], for two different ellipticity values. The laser intensity for He is 8×10^{14} W cm^{-2} and for Kr 1.2×10^{14} W cm^{-2}.

One sees from figure 5 that the tunneling exit velocity is not a universal constant, since it is clearly different for He or for Kr. For He, the velocity distributions have two well separated peaks at about ± 0.8 a.u. Recall that for elliptically polarized laser fields, tunneling ionization happens twice per optical cycle around the times when the field along the major polarization direction (x direction here) is maximum. In contrast, for Kr, the two momentum peaks can barely be distinguished due to very small absolute values.

From the VD method, it is not surprising that experiments using different atomic targets and laser parameters give different results on the tunneling exit velocity. The tunneling exit velocity is not a (zero or nonzero) constant for different atoms or laser parameters. The two experiments by Pfeiffer *et al* [34] and by Sun *et al* [37] do not contradict each other.

The numerical results from the VD method, however, do not support the assumption used in [34–37] that the tunneling exit velocity has a Gaussian distribution centered at zero with some finite width. The velocity distributions obtained by the VD method, as seen from figure 5, do not have a Gaussian shape centered at zero. Instead, they have two sharp peaks centered away from zero, especially in the He case. If a zero-centered Gaussian distribution is assumed, the width may have to be wide enough to cover the velocity magnitude as found in the VD method, in order to have the best agreement with the experimental data.

5. Summary

In this article we have given an introduction to the VD method, which is formulated with the goal of reducing the computational load of calculating wave function evolution in strong laser fields [27]. In contrast to traditional methods that calculate or approximate the wave function until the end of the laser pulse using a large numerical grid and then extracting information from the final wave function, the VD method seeks the possibility of extracting desired information, e.g., the differential momentum distribution of the particle, long before the end of the pulse. If this is possible, then further evolution of the wave function will not be needed and the computational load can be greatly reduced.

We mathematically prove in this article that in the asymptotic limit where the wave packet can be regarded as free, the differential momentum distribution obtained by the VD method, a scheme that resembles real detection processes, is equivalent to Fourier transforming the wave packet. This is the first time that such a mathematical proof is given, and this proof is the theoretical basis of the VD method.

In the opposite limit of putting the VDs in the vicinity of the interaction center, the VD method has been found useful in extracting dynamical information about the tunneling ionization process [29–33, 57]. We believe that the VD method provides conceptually the most straightforward quantum mechanical definitions to some physical quantities of interest, such as the tunneling delay time and the velocity at the tunneling exit. These quantities are raised not only by pure theoretical curiosity, but also by real experiments [34–37, 51–54].

Acknowledgments

We acknowledge funding support from China Science Challenge Project No. TZ2018005, China NSF No. 11774323, NSAF No. U1730449, National Key R&D Program No. 2017YFA0403200, and US Department of Energy Grant No. DE-FG02-05ER15713.

ORCID iDs

Xu Wang https://orcid.org/0000-0002-8043-7135

References

[1] Kulander K C, Schafer K J and Krause J L 1993 *Super-Intense Laser-Atom Physics* ed B Piraux, A L'Huillier and K Rzazewski (New York: Plenum)
[2] Corkum P B 1993 *Phys. Rev. Lett.* **71** 1994
[3] McPherson A, Gibson G, Jara H, Johann U, Luk T S, McIntyre I A, Boyer K and Rhodes C K 1987 *J. Opt. Soc. Am.* B **4** 595
[4] Ferray M, L'Huillier A, Li X F, Lompre L A, Mainfray G and Manus C 1988 *J. Phys.* B **21** L31
[5] Walker B, Sheehy B, DiMauro L F, Agostini P, Schafer K J and Kulander K C 1994 *Phys. Rev. Lett.* **73** 1227
[6] Palaniyappan S, DiChiara A, Chowdhury E, Falkowski A, Ongadi G, Huskins E L and Walker B C 2005 *Phys. Rev. Lett.* **94** 243003
[7] Blaga C I, Xu J, DiChiara A D, Sistrunk E, Zhang K, Agostini P, Miller T A, DiMauro L F and Lin C D 2002 *Nature* **483** 194
[8] Wolter B *et al* 2016 *Science* **354** 308
[9] Brabec T and Krausz F 2000 *Rev. Mod. Phys.* **72** 545
[10] Becker W, Liu X, Ho P J and Eberly J H 2012 *Rev. Mod. Phys.* **84** 1011
[11] Krausz F and Ivanov M 2009 *Rev. Mod. Phys.* **81** 163
[12] Tong X M and Chu S-I 1997 *Chem. Phys.* **217** 119
[13] Morishita T, Chen Z, Watanabe S and Lin C D 2007 *Phys. Rev.* A **75** 023407
[14] Xiong W, Geng J, Tang J, Peng L and Gong Q 2014 *Phys. Rev. Lett.* **112** 233001
[15] Xu R, Chen Y, Liu J and Fu L 2016 *Phys. Rev.* A **94** 063417
[16] Parker J, Taylor K T, Clark C W and Blodgett-Ford S 1996 *J. Phys.* B **29** L33
[17] Parker J S, Doherty B J S, Taylor K T, Schultz K D, Blaga C I and DiMauro L F 2006 *Phys. Rev. Lett.* **96** 133001
[18] Schneider B I, Collins L A and Hu S X 2006 *Phys. Rev.* E **73** 036708
[19] Hu S X 2010 *Phys. Rev.* E **81** 056705
[20] Liu A and Thumm U 2015 *Phys. Rev. Lett.* **115** 183002
[21] Volkov D M 1935 *Z. Phys.* **94** 250
[22] Tao L and Scrinzi A 2012 *New J. Phys.* **14** 013021
[23] Scrinzi A 2012 *New J. Phys.* **14** 085008
[24] Torlina L and Smirnova O 2012 *Phys. Rev.* A **86** 043408
[25] Kaushal J and Smirnova O 2013 *Phys. Rev.* A **88** 013421
[26] Torlina L *et al* 2015 *Nat. Phys.* **11** 503
[27] Feuerstein B and Thumm U 2003 *J. Phys.* B **36** 707
[28] Wang X, Tian J and Eberly J H 2013 *Phys. Rev. Lett.* **110** 243001
[29] Teeny N, Yakaboylu E, Bauke H and Keitel C H 2016 *Phys. Rev. Lett.* **116** 063003
[30] Teeny N, Keitel C H and Bauke H 2016 *Phys. Rev.* A **94** 022104
[31] Ni H, Saalmann U and Rost J M 2016 *Phys. Rev. Lett.* **117** 023002
[32] Ni H, Saalmann U and Rost J M 2018 *Phys. Rev.* A **97** 013426
[33] Tian J, Wang X and Eberly J H 2017 *Phys. Rev. Lett.* **118** 213201
[34] Pfeiffer A N, Cirelli C, Landsman A S, Smolarski M, Dimitrovski D, Madsen L B and Keller U 2012 *Phys. Rev. Lett.* **109** 083002
[35] Hofmann C, Landsman A S, Cirelli C, Pfeiffer A N and Keller U 2013 *J. Phys.* B **46** 125601
[36] Hofmann C, Landsman A S, Zielinski A, Cirelli C, Zimmermann T, Scrinzi A and Keller U 2014 *Phys. Rev.* A **90** 043406
[37] Sun X, Li M, Yu J, Deng Y, Gong Q and Liu Y 2014 *Phys. Rev.* A **89** 045402
[38] Brabec T, Ivanov M Y and Corkum P B 1996 *Phys. Rev.* A **54** R2551
[39] Chen J, Liu J, Fu L B and Zheng W M 2000 *Phys. Rev.* A **63** 011404
[40] Yudin G L and Ivanov M Y 2001 *Phys. Rev.* A **63** 033404
[41] Quan W *et al* 2009 *Phys. Rev. Lett.* **103** 093001
[42] Smolarski M, Eckle P, Keller U and Dörner R 2010 *Opt. Express* **18** 17640
[43] Cai J, Chen Y, Xia Q, Ye D and Fu L 2017 *Phys. Rev.* A **96** 033413
[44] Li X, Wang C, Yuan Z, Ye D, Ma P, Hu W, Luo S, Fu L and Ding D 2017 *Phys. Rev.* A **96** 033416
[45] Wyatt R E 2005 *Quantum Dynamics with Trajectories: Introduction to Quantum Hydrodynamics* (Berlin: Springer)
[46] Bohm D 1952 *Phys. Rev.* **85** 166
[47] Bohm D 1952 *Phys. Rev.* **85** 180
[48] Madelung V E 1926 *Z. Phys.* **40** 322
[49] Takabayasi T 1954 *Prog. Theor. Phys.* **11** 341
[50] For example Cohen-Tannoudji C, Diu B and Laloë F 1977 *Quantum Mechanics* (Paris: Hermann) ch 7
[51] Eckle P, Pfeiffer A N, Cirelli C, Staudte A, Dörner R, Muller H G, Bütiker M and Keller U 2008 *Science* **322** 1525
[52] Landsman A S, Weger M, Maurer J, Boge R, Ludwig A, Heuser S, Cirelli C, Gallmann L and Keller U 2014 *Optica* **1** 343
[53] Camus N, Yakaboylu E, Fechner L, Klaiber M, Laux M, Mi Y, Hatsagortsyan K Z, Pfeifer T, Keitel C H and Moshammer R 2017 *Phys. Rev. Lett.* **119** 023201
[54] Sainadh U S *et al* 2017 arXiv:1707.05445
[55] Goreslavsky S P and Popruzhenko S V 1997 *Laser Phys.* **7** 700
[56] Arissian L, Smeenk C, Turner F, Trallero C, Sokolov A V, Villeneuve D M, Staudte A and Corkum P B 2010 *Phys. Rev. Lett.* **105** 133002
[57] Wang J and He F 2017 *Phys. Rev.* A **95** 043420